How does the Bax-α1 targeting sequence interact with mitochondrial membranes? The role of cardiolipin

ARTICLE *in* BIOCHIMICA ET BIOPHYSICA ACTA · FEBRUARY 2009

Impact Factor: 4.66 · DOI: 10.1016/j.bbamem.2008.12.014 · Source: PubMed

3 AUTHORS:

Marc-Antoine Sani
University of Melbourne
42 PUBLICATIONS **378** CITATIONS
SEE PROFILE

Erick Dufourc
University Bordeaux, CNRS, Bordeaux INP
171 PUBLICATIONS **4,210** CITATIONS
SEE PROFILE

Gerhard Gröbner
Umeå University
100 PUBLICATIONS **2,052** CITATIONS
SEE PROFILE

Biochimica et Biophysica Acta 1788 (2009) 623–631

Contents lists available at ScienceDirect

Biochimica et Biophysica Acta

journal homepage: www.elsevier.com/locate/bbamem

How does the Bax-α1 targeting sequence interact with mitochondrial membranes? The role of cardiolipin

Marc-Antoine Sani [a,b], Erick J. Dufourc [a,*], Gerhard Gröbner [b,*]

[a] UMR 5248 CBMN, CNRS, Université Bordeaux 1, ENITAB, IECB, 33607 Pessac Cedex, France
[b] Department of Chemistry, Umeå University, 90187 Umeå, Sweden

ARTICLE INFO

Article history:
Received 7 August 2008
Received in revised form 19 November 2008
Accepted 18 December 2008
Available online 7 January 2009

Keywords:
Apoptosis
Bax N-terminal
Cardiolipin
Solid-State NMR

ABSTRACT

A key event in programmed cell death is the translocation of the apoptotic Bax protein from the cytosol towards mitochondria. The first helix localized at the N-terminus of Bax (Bax-α1) can act here as an addressing sequence, which directs activated Bax towards the mitochondrial surface. Solid state NMR (nuclear magnetic resonance), CD (circular dichroism) and ATR (attenuated total reflection) spectroscopy were used to elucidate this recognition process of a mitochondrial membrane system by Bax-α1. Two potential target membranes were studied, with the outer mitochondrial membrane (OM) mimicked by neutral phospholipids, while mitochondrial contact sites (CS) contained additional anionic cardiolipin. ^{1}H and ^{31}P magic angle spinning (MAS) NMR revealed Bax-α1 induced pronounced perturbations in the lipid headgroup region only in presence of cardiolipin. Bax-α1 could not insert into CS membranes but at elevated concentrations it inserted into the hydrophobic core of cardiolipin-free OM vesicles, thereby adopting β-sheet-like features, as confirmed by ATR. CD studies revealed, that the cardiolipin mediated electrostatic locking of Bax-α1 at the CS membrane surface promotes conformational changes into an α-helical state; a process which seems to be necessary to induce further conformational transition events in activated Bax which finally causes irreversible membrane permeabilization during the mitochondrial apoptosis.

1. Introduction

Programmed cell death is essential for the regulation of cell homeostasis in complex organisms. Failures in this physiological regulation trigger severe pathological diseases including autoimmune disorders, neuro-degeneration and cancer [1–3]. Induction of apoptosis via the mitochondrial pathway is mainly controlled by the Bcl-2 protein family which is made up of three different groups of proteins: the anti-apoptotic proteins including Bcl-2, all with four Bcl-2 homology domains (BH1–4); the pro-apoptotic proteins such as Bax with three Bcl-2 homology domains (BH1–3); and the BH3-only proteins like Bid or Bad, which can activate pro-apoptotic proteins or inhibit anti-apoptotic proteins activities [4–6]. The interplay between these different protein fractions regulates the permeability of the mitochondrial membrane system, and in particular any release of apoptotic activator factors such as cytochrome *c*, which reside between the outer (OM) and the inner (IM) membranes of the mitochondrion [7–9].

While anti-apoptotic proteins are originally anchored in the outer mitochondrial membrane, the main pro-apoptotic protein, Bax, is located in the cytosol in an inactive form [10–12]. However, binding of an external apoptotic stimulus – often BH3 only proteins – to Bax protein will induce a conformational change into its active conformation. This process will expose Bax targeting/anchoring domains, thereby forcing its translocation to the mitochondria membrane, where it can exert its apoptotic role [10,12–14]. It has been proposed that the first helix localized at the N-terminal of the Bax protein is an effective addressing sequence because its deletion prevents Bax localization into mitochondria while the very first amino acids are an inhibitory sequence [14,15]. However, debate exists on which of the N-terminus or the C-terminus, or both of them, are required for the protein localization at the OM system [16,17]. Furthermore, the mechanism by which Bax induces the release of apoptotic factors is controversial, involving different locations of Bax activity and therefore an important role of the mitochondrial membrane composition. Especially, the role of cardiolipin, a mitochondrion specific phospholipid, for Bax functioning is hardly discussed but a recent study showed its importance for Bax targeting towards and functioning at mitochondrial membrane surface [18]. The Bax specific recognition prior activation of the mitochondrial membrane is still not understood and in order to address this question one clearly has to know how and where the activated Bax protein does target the complex mitochondrial membrane system.

* Corresponding authors. G. Gröbner is to be contacted at Department of Chemistry, Umeå University, 901 87 Umeå, Sweden. Tel.:/fax: +46 907866346/7779. E. J. Dufourc, UMR 5248 CBMN CNRS, Université Bordeaux 1, ENITAB, IECB 2 rue Robert Escarpit, 33607 Pessac, France. Tel.:/fax: +33 5 4000 2218.
E-mail addresses: e.dufourc@iecb.u-bordeaux.fr (E.J. Dufourc), gerhard.grobner@chem.umu.se (G. Gröbner).

0005-2736/$ – see front matter © 2008 Elsevier B.V. All rights reserved.
doi:10.1016/j.bbamem.2008.12.014

Using several biophysical techniques, solid state NMR (nuclear magnetic resonance), CD (circular dichroism) and ATR (attenuated total reflection) spectroscopy, we investigated the interactions between the supposed addressing sequence, the first helix of Bax (Bax-α1), (^{14}TSSEQIMKTGALLLQGFIQDRAGRM^{38}), with two potential target models — outer membrane (OM) *versus* contact site (CS) mimicking vesicles. The OM membrane is mainly composed of neutral phosphatidylcholine and phosphatidylethanolamine lipids [19]. However, contact sites which reside between the inner and the outer membranes, are known to be highly enriched in the anionic phospholipid cardiolipin [20]. Depending on the target membrane, we observed two different interaction mechanisms (electrostatically driven *versus* hydrophobically driven) and membrane specific structural changes in the Bax-α1 peptide; information that is useful to elucidate the potential role of cardiolipin in the Bax addressing process.

2. Experimental procedures

2.1. Materials

1-Palmitoyl-2-Oleoyl-*sn*-Glycero-3-Phosphocholine (POPC), 1-Palmitoyl-2-Oleoyl-*sn*-Glycero-3-Phosphoethanolamine (POPE), heart cardiolipin and chain deuterated 1-Palmitoyl ($^2H_{31}$)-2-Oleoyl-*sn*-Glycero-3-Phosphocholine ($^2H_{31}$-POPC) were purchased from Avanti Polar Lipids (Alabama, USA). The Bax-α1 peptide (^{14}TSSEQIMKTGALLLQGFIQDRAGRM^{38}) from the Bax human protein was synthesized by solid phase methods on an Applied Biosystems 433A Peptide Synthesizer (PE Biosystem, Courtaboeuf, France) [21]. The peptide purity was greater than 98% as controlled by UV and MALDI-TOF mass spectrometry.

2.2. Circular dichroism (CD)

The lipids were dissolved in $CHCl_3$/CH_3OH (3:1 v/v) at the desired molar ratio and the solvent removed under vacuum. The lipid films were then re-suspended in water, followed by a lyophilization step. The fluffy lipid powders were finally re-suspended in a 20 mM HEPES buffer (pH 7) containing 150 mM NaCl salt to reach a concentration of 3 mM. Small unilamellar vesicles (SUV) were prepared by sonication using a tip sonicator (Soniprep 150, MSE, Tokyo, Japan). CD-spectra (Jasco J-810 spectropolarimeter, USA) of peptide solutions were recorded between 190–250 nm using a 1 mm path-length quartz cell (Hellma, Germany). Samples were allowed to equilibrate 15 min at 35 °C prior to accumulation of 8 scans. The lipid background was subtracted. To estimate the peptide secondary structure content, an analysis of the relevant CD-spectra was carried out using the CDPro software (http://lamar.colstate.edu/~ssreeram/CDPro) developed by R. W. Woody and coworkers [22]. CD values were converted to mean residue ellipticity (MRE). The basis set 10 of the CDPro software was used [23]. Analysis was performed using three methods, CONTIN, CONTIN/LL, and SELCON 3 [23,24]. In general, CONTIN/LL, a self-consistent method with an incorporated variable selection procedure, produced the most reliable results.

2.3. Solid state nuclear magnetic resonance spectroscopy (NMR)

As described before, fluffy lipid powder mixtures were resuspended in identical HEPES buffer (pH 7) containing the desired amount of peptide to obtain 20:1 or 50:1 lipid-to-protein (L/P) molar ratios, and freeze-dried overnight. For ^{1}H NMR and ^{31}P NMR experiments, each sample (*ca.* 15 mg of lipids) was re-suspended in 45 μL of ^2H_2O at a final hydration of 75% [(mass of water)/(mass of lipids and water), in percent], followed by three freeze–thaw cycles to homogenize the multilamellar vesicle sample. For ^{2}H NMR, 1 mg of $^2H_{31}$-POPC was added to each previous sample, followed by five freeze–thaw cycles and freeze-drying overnight. Each sample was finally re-suspended in 45 μL deuterium-depleted water and homogenized.

^{1}H NMR and ^{31}P NMR measurements were carried out on a 400 MHz Infinity spectrometer (Chemagnetics, USA) with a 4 mm double resonance CP-MAS probe. ^{1}H NMR experiments were acquired by using a single π/2-pulse *of* 6 μs duration and a repetition delay of 3 s at a magic angle spinning speed of 6 kHz. Spectra were referenced by setting the water signal to 4.7 ppm. ^{31}P MAS NMR experiments were acquired under continuous wave proton decoupling (40 kHz) using a single π/2-pulse with 7 μs duration at spinning speed of 6 kHz [25]. A Hahn-echo pulse sequence was applied for static ^{31}P NMR measurements with an interpulse delay of 50 μs and a Lorentzian line broadening of 100 Hz was used prior to Fourier transformation. All ^{31}P NMR spectra were referenced externally to −0.9 ppm, using DMPC vesicles at 35 °C. 100 to 15000 transients were co-added with a repetition time of 3 s.

^{2}H NMR experiments were performed at 76.77 MHz on a Bruker Avance DSX 500. A quadrupole echo pulse sequence (π/2-τ-π/2-τ-acquisition) [26] was used with an interpulse delay τ of 30 μs. The 90° pulse length was 3 μs and the repetition time 1.5 s. 8 k acquisitions were typically recorded and a Lorentzian line broadening of 200 Hz was used prior to Fourier transformation. Spectra were acquired at 35 °C and 25 °C; the temperature was regulated to ±1 °C. Samples were allowed to equilibrate for 30 min between each temperature before the NMR signal was acquired.

2.4. Polarized attenuated total reflection spectroscopy (ATR)

ATR spectra were recorded on a Nicolet Magna 550 spectrometer (Ramsey, Minnesota, USA), equipped with a MCT detector cooled to 77 K, where the sample as used for NMR was sheared at the diamond ATR crystal surface (golden gate, Eurolabo, France). Deconvolution of the ATR spectra was done using Grams 32 software (Thermo electron). Because ATR spectroscopy is sensitive to the orientation of structures, spectra were recorded with a parallel (p) and perpendicular (s) polarization of the incident light with respect to the ATR plate [27,28]. All the orientational information is then contained in the dichroic ratio $R_{ATR}=A_p/A_s$, where A_i represents the absorbance of the considered band for the p or s polarization of the incident light, respectively [29,30]. Generally 1000 scans were accumulated at a resolution of 8 cm^{-1} and a two-level zero filling was performed.

3. Results

CD and ATR spectroscopies were used to monitor conformational changes in the Bax-α1 domain upon its association to outer membrane (OM) and contact site (CS) membrane mimicking systems. The ion strength was varied to elucidate the contribution of electrostatics to the membrane affinity of the Bax-α1 peptide. ^{1}H MAS NMR was applied to follow changes across the whole lipid bilayer whereas wideline and MAS ^{31}P NMR provided a picture of peptide-induced structural and dynamical perturbations in the lipid headgroup region. Finally, changes in the hydrophobic core of the membrane were monitored by using deuterium-labeled POPC and ^{2}H NMR.

3.1. Secondary structure of Bax-α1 upon titration with OM or CS mimicking lipid vesicles

Membrane-mediated conformational behavior of Bax-α1 was characterized by circular dichroism (CD). For this purpose peptide at a fixed 20 μM concentration in buffer solution was titrated with small unilamellar vesicles (SUV) composed either of POPC/POPE (65:35, molar ratio) mimicking the outer membrane (OM) or POPC/POPE/CL (43:36:21, molar ratio) mimicking the contact sites (CS) of

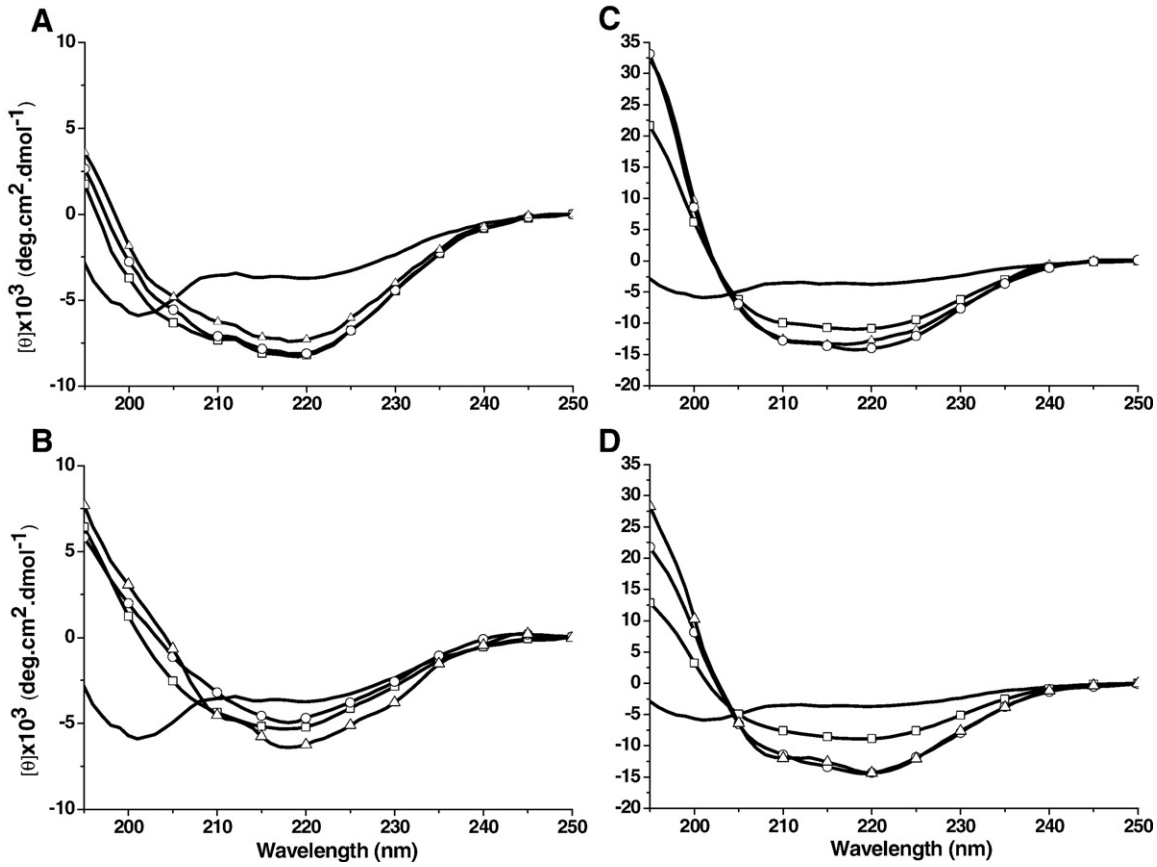

Fig. 1. CD spectra of Bax-α1 peptide (20μM) at 35 °C upon titration by vesicles composed of POPC/POPE (65:35, molar ratio) at 1 mM NaCl (A) and 50 mM of NaCl (B); by vesicles composed of POPC/POPE/CL (43:36:21, molar ratio) with 1 mM of NaCl (C) and 50 mM NaCl (D) present. The lipid to peptide molar ratios (L/P) depicted in the four panels are 100 (triangle), 50 (circle), 20 (square) and pure peptide in HEPES buffer at pH 7 (solid line).

mitochondria. Two different salt concentrations were used, 1 mM or 50 mM, in order to investigate the binding strength of Bax-α1 onto membranes.

In the absence of vesicles, Bax-α1 displays a partition between random coil (40%) and β-sheet structures (30%) in HEPES buffer solution (1 mM NaCl present). This is close to the behavior reported in our previous study, which however used a different buffer and a higher peptide concentration, both promoting a slightly higher random coil content [21]. Addition of POPC/POPE SUV to Bax-α1 at low ionic strength, induces weak changes, mainly aggregation as β-sheet structures, with the characteristic low intensities of a broad minimum at ca 218 nm and a maximum at ca 195 nm (Fig. 1 panel A), as seen for amyloid-beta peptide [31]. The β-sheet content reaches its maximum value (47%) at L/P 100:1 (Table 1). Increase in ionic strength does not change significantly the peptide structural behavior during titration with neutral lipid vesicles (Fig. 1, panel B). Upon titration with CS mimicking lipid vesicles, the peptide undergoes a strong conformational transition into dominant helical features with the typical minima at 222 and 208 nm and a maximum at ca.190 nm (see Fig. 1, panel C). The maximum amount of helical structure is obtained at a L/P molar ratio of 50:1 with 47±5% of α-helix (see Table 1). As shown in Fig. 1 (panel D), the presence of NaCl at 50 mM has no pronounced consequences in the peptide structural behavior upon titration.

3.2. ^{1}H MAS NMR on OM and CS multilamellar vesicles interacting with Bax-α1

^{1}H MAS NMR was applied to monitor the degree of perturbation across the whole membrane, as reflected in the different molecular segments of the lipid molecules: hydrophobic chains and headgroup region. ^{1}H MAS NMR results for Bax-α1 interacting with the two different vesicle systems are shown in Fig. 2 where signals arising from headgroups region (A, C panels) and those arising from the acyl chains region (B, D panels) are separately displayed. Adding the peptide to OM mimicking vesicles induces two new components at 1.12 ppm and 1.53 ppm, while no additional spectral components or severe modifications are visible in CS mimicking vesicles. The effect is

Table 1
Secondary structure of the Bax-α1 peptide[a] upon titration by POPC/POPE or POPC/POPE/CL SUV[b] containing 1 mM (50 mM)[c] of NaCl

	L/P	α Helix[d] (%)	β Sheet[d] (%)	β Turn[d] (%)	Random coil[d] (%)
HEPES buffer pH 7		6	28	22	44
POPC/POPE (65:35, molar ratio)					
	20	10 (*9*)	32 (*31*)	22 (*39*)	36 (*21*)
	50	12 (*5*)	38 (*43*)	22 (*21*)	28 (*31*)
	100	10 (*8*)	47 (*44*)	20 (*21*)	23 (*27*)
POPC/POPE/CL (43:36:21, molar ratio)					
	20	33 (*19*)	20 (*27*)	19 (*22*)	28 (*32*)
	50	47 (*36*)	13 (*16*)	16 (*18*)	24 (*30*)
	100	42 (*42*)	14 (*18*)	15 (*6*)	28 (34)

Accuracy is estimated to be 5% for 1 mM of NaCl.
[a] Concentration fixed at 20 μM.
[b] SUV obtained by sonication.
[c] (−) in buffer containing 50 mM NaCl.
[d] Deconvolution of CD spectra was accomplished using basis 10 from the CDPro software and the CONTIN/LL algorithm[51; 53; 58].

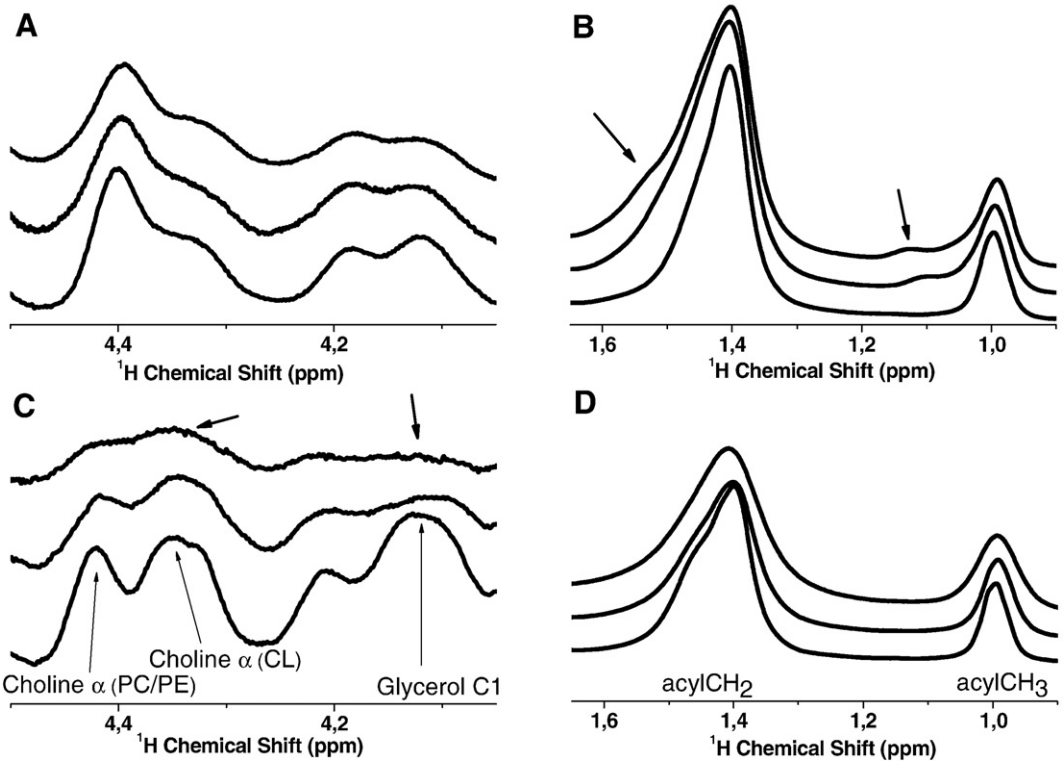

Fig. 2. ^{1}H MAS NMR spectra at 6 kHz spinning speed at 35 °C of multilamellar vesicles composed of POPC/POPE (65:35, molar ratio) in HEPES buffer (pH 7, 75% hydration): headgroup region (A) and acyl chain region (B); and of POPC/POPE/CL (43:36:21, molar ratio): headgroup region (C) and acyl chain region (D). Pure MLVs (bottom spectrum); Bax-α1 added at a 50:1 L/P (middle spectrum) and at a 20:1 L/P molar ratios (top spectrum).

more pronounced at 20:1 L/P molar ratio. In contrast, the peptide does not disturb significantly the headgroup region of OM mimicking vesicles while severe broadening and intensity loss appear in the CS mimicking vesicles with a remarkable effect on the glycerol C1 resonance (4.35 ppm) and especially on the choline α of cardiolipin (4.12 ppm). Again, the broadening effect is more pronounced at 20:1 L/P molar ratio.

3.3. Bax-α1 strongly binds to negatively charged membrane surfaces

In order to investigate in more detail the structural and dynamical changes in the lipid headgroup region when Bax-α1 is approaching the mitochondrial membrane interfaces, wideline and high resolution MAS solid state ^{31}P NMR spectroscopy was carried out on mitochondrial OM and on CS mimicking multilamellar membrane models. In Fig. 3 (left panel), wideline ^{31}P NMR spectra of OM vesicles exhibit a typical pattern of lipid bilayers in a fluid lamellar phase with axial symmetry before and upon addition of Bax-α1 peptide at 35 °C. Because the phosphate groups in POPC and POPE possess distinct chemical shift anisotropy (CSA) values, the lineshape exhibits superimposed spectra arising from both lipids with well resolved 90° ($\sigma_\perp$) and 0° ($\sigma_{//}$) edges, giving a CSA value ($\sigma_{//}$–$\sigma_\perp$) of ca. 45 and 36 ppm, respectively. Addition of Bax-α1 peptide does not change significantly the CSA at any L/P molar ratio investigated but a small loss in the 90° edge resolution and a higher intensity in the 0° edge occur as often reported from the onset of low frequency membrane motions as promoted by membrane proteins [32,33].

The lipid MLVs containing cardiolipin produce the same typical NMR lineshapes of a lamellar membrane phase as clearly seen in Fig. 2 (right panel). Once again, POPC, POPE and cardiolipin contribute to the total lineshape but a broadening of the whole spectrum is observed, making a separate characterization of the CSA for each lipid component delicate. The presence of cardiolipin clearly induces a marked change in mobility/orientation of the headgroup region as seen in the reduction of CSA to ca. 27 ppm (left panel, bottom line). Addition of Bax-α1 produces a further decrease in CSA down to 26 ppm at a 50:1 L/P and to 25 ppm at 20:1 L/P molar ratios. The lineshape is noticeably modified with the 0° edge resolution diminished and a reduction in the 90° edge. With the decrease of L/P ratio, the spectra are more and more broadened which might be due to severe changes in the transverse relaxation T_2 (onset of slow motions as lipid diffusion or collective membrane motion), as reported for cationic peptide interacting with membrane [34].

To observe peptide induced changes for each lipid component separately, high resolution ^{31}P MAS NMR was performed, where the

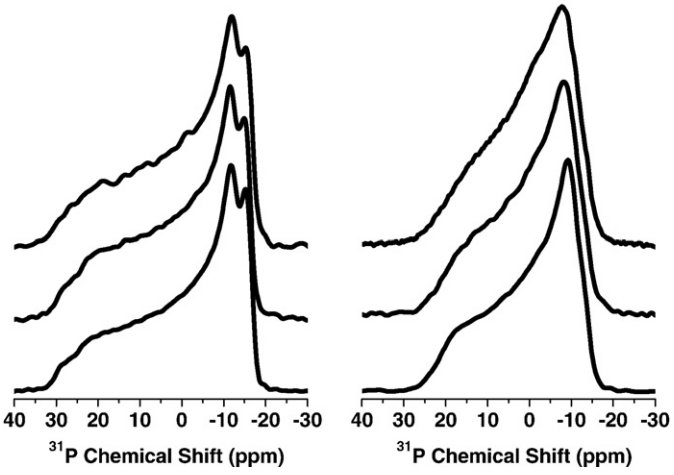

Fig. 3. Static ^{31}P NMR spectra of peptide-free MLVs composed of POPC/POPE (65:35, molar ratio) mimicking the outer membrane composition (left panel) and of POPC/POPE/CL (43:36:21, molar ratio) mimicking the contact site composition (right panel) at 35 °C in HEPES buffer (pH 7, 75% hydration). Pure MLVs (bottom) with Bax-α1 added at a 50:1 L/P (middle) and at a 20:1 L/P molar ratios (top).

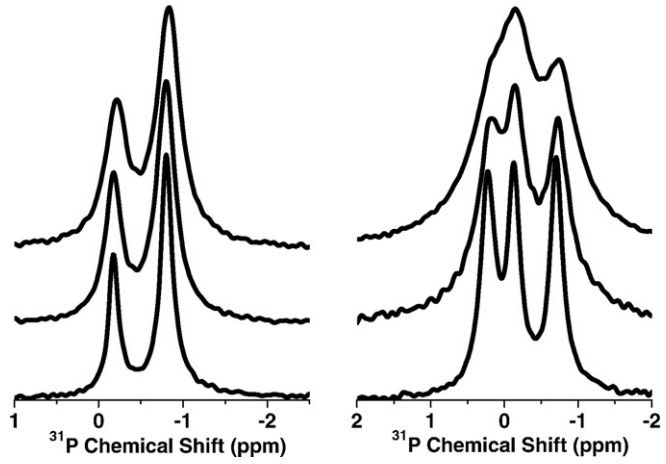

Fig. 4. ^{31}P MAS NMR spectra at 6 kHz spinning speed at 35 °C for peptide-free MLVs composed of POPC/POPE (65:35, molar ratio) mimicking the outer membrane composition (left panel) and of POPC/POPE/CL (43:36:21, molar ratio) mimicking the contact site composition (right panel) in HEPES buffer (pH 7, 75% hydration). Pure MLVs (bottom) with Bax-α1 added at a 50:1 L/P (middle) and at a 20:1 L/P molar ratios (top).

PC, PE and CL phosphate signals are separated by their different isotropic chemical shift (σ_i) values. At 6 kHz spinning speed, the CSAs for all lipids are entirely averaged out and only isotropic chemical shift contributions are visible as seen in Fig. 4. The resonances (σ_i) of the OM vesicles are −0.81 ppm and −0.18 ppm for POPC and POPE, respectively. At L/P 50, there is no change in the σ_i for both lipids but a slight upfield shift occurs at L/P 20 to −0.85 ppm and −0.21 ppm, respectively. However, the linewidth (FWHH) is broadened with increase of the peptide amount (see Table 2). The lipid molar ratio (65:35) between the integrals of isotropic resonances is nearly constant independently of the L/P molar ratio.

Because incorporation of cardiolipin increases the negative surface potential of the membrane, in the absence of peptide, a typical upfield shift occurs as described previously [25]. Indeed, three isotropic chemical shifts can be resolved at −0.71, −0.14 and 0.21 ppm corresponding to POPC, POPE and cardiolipin, respectively, with areas representative of the molar ratios 43:36:21. In the presence of Bax-α1 at a 50:1 L/P molar ratio, the deconvolution of the spectrum required addition of a broad fourth component (see supplementary material, Fig. S1). This required fourth component has been described previously as a lipid pool reflecting the overlapped spectral contribution from the lipids proportion interacting with the peptide [35]. It is not well understood yet, but one can see it as lipid complexed with the peptide (overlapped components) while part of the lipids remains unperturbed. The σ_i are approximately identical as for the free-peptide vesicles, the fourth component is sitting at −0.26 ppm (see Table 2). From the deconvolution, the composition of the fourth component would represent 33% of the total area. The FWHHs are greatly affected by the presence of the peptide, as seen in Table 2, with a higher broadening occurring for the cardiolipin. Addition of further peptide (L/P 20:1) increases significantly this effect, by even reducing further the σ_i to −0.78 (POPC), −0.15 (POPE) and particularly the cardiolipin to 0.11 ppm, while the fourth component is shifted upfield to −0.22 ppm. Again, the FWHHs are considerably increased, especially for cardiolipin, while approximately constant for the fourth component (see Table 2). Interestingly, the area of this latter increased consequently, corresponding to 60% of the whole spectrum which supports the idea of partition between peptide-free and peptide-interacting lipid pools. Indeed, the cardiolipin depletion in the peptide-free lipid pool would move towards neutral membrane potential as reflected in the chemical shift and the opposite for the peptide-interacted lipid pool, nevertheless with less effect due to the peptide potential compensation.

3.4. Cardiolipin prevents deep insertion of Bax-α1 into the hydrophobic membrane core

To monitor the impact of Bax-α1 on the lipid hydrophobic core, we incorporated a small fraction (6.7%) of $^2H_{31}$-POPC lipid into these model bilayers. Although these NMR spectra are difficult to acquire, this procedure induced only very minor modification to the lipid/lipid and lipid/peptide initial ratios and the physico-chemical behavior of theses membranes. Pure spectra of $^2H_{31}$-POPC MLV were compared to the peptide-free ones (cardiolipin-containing or not) to check whether the deuterated lipid was well incorporated. Results (spectra not shown) lead to much lower splittings for pure $^2H_{31}$-POPC liposomes (23 kHz and 2.1 kHz for "plateau" – labeled carbon positions 2–8, near the interface – and chain end – methyl terminal at C16 – regions, respectively) than with POPC/POPE or POPC/POPE/CL containing MLV (see Fig. 5) and no overlap could be noticed meaning that no pure POPC liposomes were coexisting in solution.

As seen in Fig. 5 (left panel), at 35 °C the POPC/POPE membrane is entirely in the L_α fluid state and exhibits fast intra- and intermolecular axially symmetric motions with defined plateau and methyl group regions. The "plateau" region has a quadrupolar splitting of ca. 27.5 kHz, and the terminal methyl group a splitting of 3.1 kHz. Addition of Bax-α1 triggers a reduction for both the "plateau", from 27.5 kHz to 26 kHz, and methyl region, from 3.1 kHz to 2.6 kHz, at L/P ratio 20:1 while ratio L/P 50:1 shows slight perturbations. Addition of cardiolipin to POPC/POPE liposomes increases the $^2H_{31}$-POPC dynamics as observed by the reduced "plateau" quadrupolar splitting of 25.5 kHz (Fig. 5, right panels). Further addition of Bax-α1 does not disturb significantly the plateau region (less than 0.5 kHz reduction for both ratios) or the methyl region (rather identical splittings). The isotropic resonance in the ^2H spectra in presence of peptide

Table 2
^{31}P MAS[a] NMR data[b] of outer membrane mimicking (POPC/POPE) or contact site mimicking (POPC/POPE/CL) MLV[c] containing different amount of Bax-α1

	Peptide-free MLVs			L/P 50			L/P 20		
	σ_i[d] (ppm)	FWHH (ppm)	Integral	σ_i[d] (ppm)	FWHH (ppm)	Integral	σ_i[d] (ppm)	FWHH (ppm)	Integral
POPC/POPE (65:35)									
POPC	−0.81	0.15	65	−0.81	0.27	65	−0.85	0.33	65
POPE	−0.18	0.14	35	−0.18	0.23	35	−0.21	0.31	35
POPC/POPE/CL (43:36:21)									
POPC	−0.71	0.20	43	−0.72	0.29	28	−0.78	0.41	18
POPE	−0.13	0.20	36	−0.13	0.27	26	−0.15	0.36	16
CL	0.22	0.23	21	0.20	0.37	13	0.11	0.49	5
4th	–	–	–	−0.26	1.37	33	−0.21	1.36	61

[a] At 6 kHz spinning speed.
[b] Deconvolution obtained from the PFM module of OriginPro 7.5 (OriginLAb corporation, USA) software, using Lorentzian function.
[c] In HEPES buffer containing 50 mM of NaCl at 75%w hydration level.
[d] Chemical shifts determined to ±0.02 ppm.

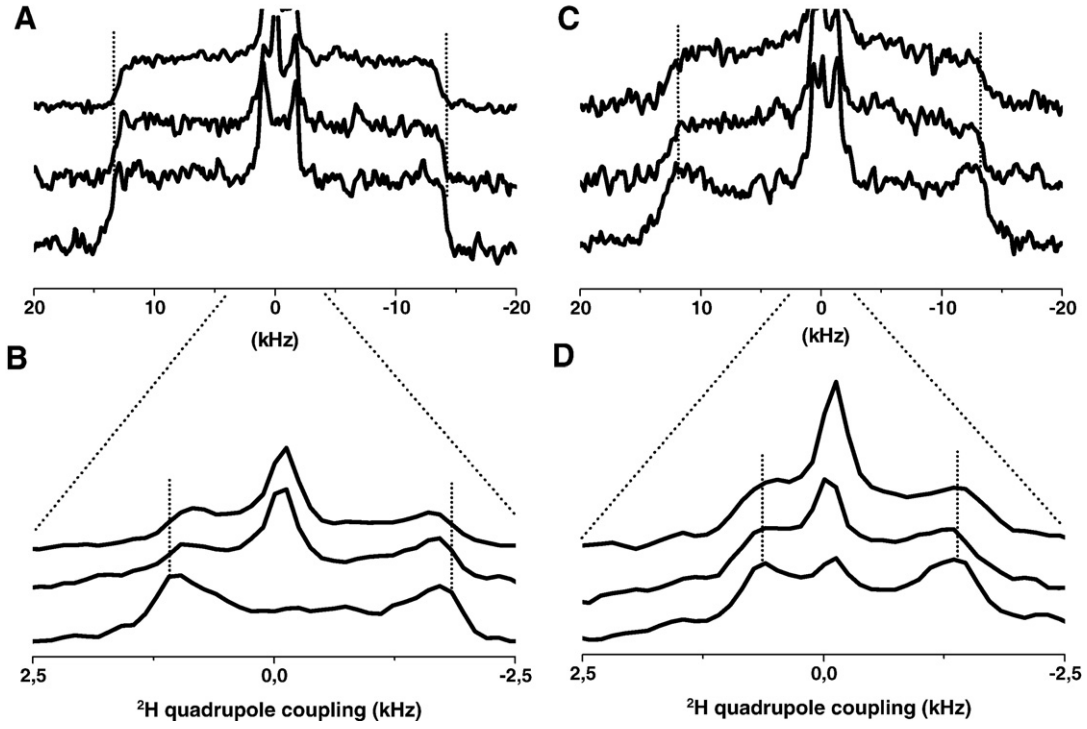

Fig. 5. Static ^{2}H NMR spectra of MLVs composed of POPC/POPE (65:35, molar ratio) (panels A, B) and of POPC/POPE/CL (43:36:21, molar ratio) (panels C, D) at 35 °C in HEPES buffer (pH 7, 75% hydration): full spectrum (top panels) and methyl group region (bottom panels). Pure MLVs (bottom spectrum) with Bax-α1 added at a 50:1 L/P (middle spectrum) and at a 20:1 L/P molar ratios (top spectrum).

contributed less than 3% of the total lineshape. This contribution might come from either small fragment during the freeze–thaw procedure or from deuteron-containing water produced by exchange with the environment. An alternative explanation such as peptide induced non-bilayer structures can be ruled out since no resonances indicative of an isotropic phase are visible in the static ^{31}P NMR spectra as seen in Fig. 3. In order to confirm further a possible insertion of Bax-1 in OM mimicking membranes, polarized ATR was performed on Bax-α1 added to oriented lipid multibilayers of POPC/POPE (65:35, molar ratio) in ratio L/P 20:1 prepared in the same way as for NMR sample (see supplementary material, Fig. S2). The main components in the amide bands at 1620 cm^{-1} and 1680 cm^{-1} are characteristic of a major anti-parallel β-sheet structure, supporting the CD data. The dichroic ratios ($R^{ATR} = \frac{A_p}{A_s}$) were used to evaluate the orientation relative to the bilayer normal. Values of 0.95±0.03 and 1.13±0.21, respectively, were found and correspond to angle values of 56°±10 relative to the bilayer normal and 40°±10 versus the β-strand axis according to Tamm et al. [30]. These values confirm the ability of Bax-1 to insert into neutral bilayer.

4. Discussion

The major outcome of our experimental findings is summarized in Fig. 6, where a molecular mechanism of Bax-α1 interacting with different mitochondrial target membranes is presented. Clearly the affinity of occurring lipid–peptide interactions depends on the membrane composition: Bax-α1 interacts with neutral membranes mimicking the outer mitochondrial membranes only at high concentration causing insertion and membrane disordering. However, cardiolipin promotes strong and preferential electrostatic interactions with Bax-α1 which is locked onto the negatively charged surface over the whole concentration range used. Bax-α1 also undergoes severe conformational changes with adoption of α-helical features if cardiolipin containing membranes are present while it slightly aggregates as anti-parallel beta sheet structure into OM membranes. All these aspects will be discussed below, with implications for the potential regulative addressing of Bax protein in the mitochondrial apoptotic pathway.

4.1. Electrostatic versus hydrophobic forces driving Bax-α1 localisation

All NMR results which were obtained for three different reporter nuclei, support a small effect of Bax-α1 peptide on neutral OM membranes except at high concentration where insertion is promoted. ^{1}H NMR and ^{2}H NMR show a perturbation in the hydrophobic region while ^{31}P NMR indicates no pronounced perturbation of the OM membrane headgroup and glycerol region. The new components at 1.12 ppm and 1.53 ppm, as seen in the ^{1}H MAS NMR spectra (Fig. 2B), most likely is caused by a close interaction between the CH_2/CH_3 region of the phospholipids and the aromatic ring of the phenylalanine residue of the peptide. This phenomenon was previously observed for DPPC liposomes interacting with tryptophan containing peptides [36]. Since no resonance at 1.12 or 1.53 ppm can be observed in POPC/POPE/cardiolipin membranes containing the same molar ratio of peptide (Fig. 2D), the possibility that the origin of the new resonances comes from methyl groups is unlikely, but instead favours the insertion of the peptide in the vicinity of the CH_2/CH_3 region of neutral membranes. Moreover, the ratio dependence of the disordering effect of the hydrophobic core, seen by the reduction of the quadrupolar splittings in ^{2}H NMR, is due to an increase of the dynamics of the acyl chains; which indicates the peptide population inserted into the membrane core without any interference with the headgroup region as our ^{31}P NMR results clearly showed (Fig. 3). This is supported by the ATR results at 20:1 L/P molar ratio that indicate an average peptide tilt inside the outer membrane core. This oblique orientation is often reported for amphipathic peptides such as antimicrobial or fusogenic peptides [37,38] and is explained by hydrophobic mismatch between the spanning peptide and the hydrophobic membrane core [39].

However, the presence of negatively charged cardiolipin to the lipid bilayers mimicking CS clearly attracts Bax-α1 onto the surface. As

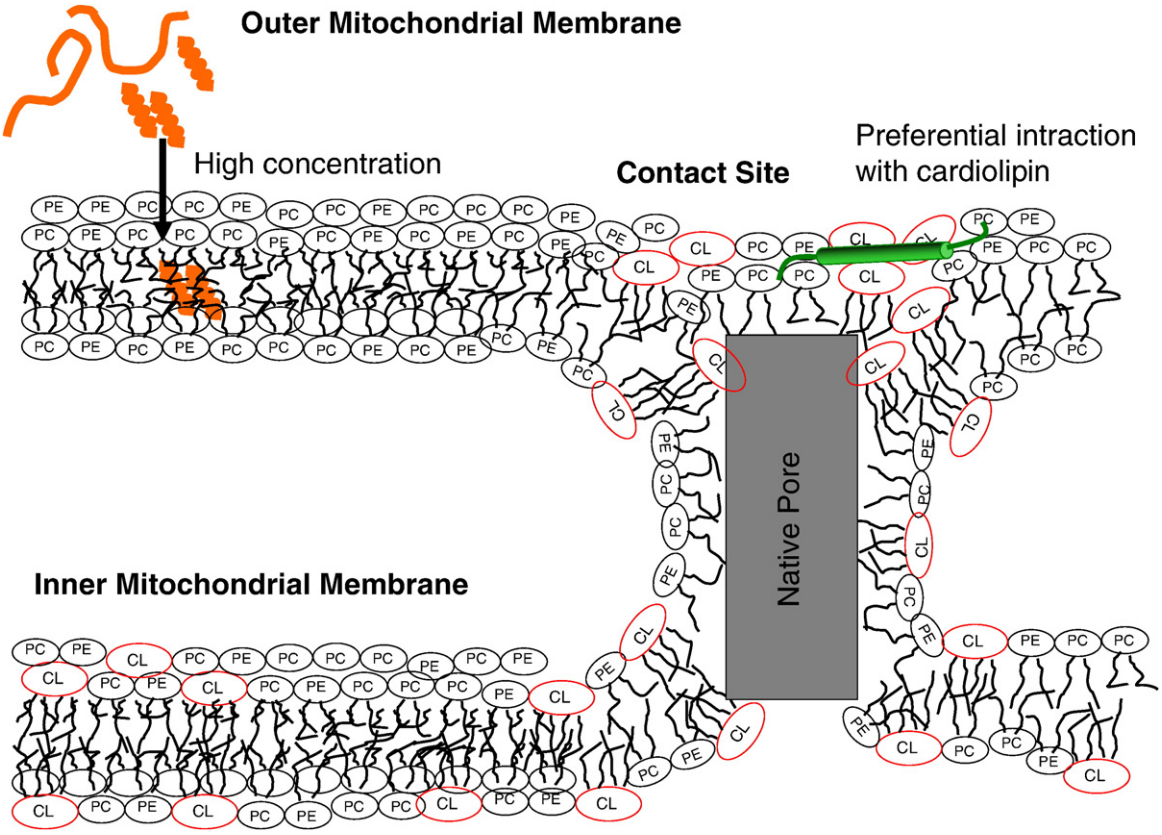

Fig. 6. Biophysical model of Bax-α1 interaction with two different mimicked mitochondrial locations. Hydrophobic interactions occurring at the outer membrane, mainly composed of neutral lipids POPC and POPE, induce partition between β-sheet inserted structures (especially at high concentration) and random coil conformation remaining in solution of Bax-α1. Contact site mimicked membrane, where native pores are stabilized (shown as an example here), are enriched by the anionic cardiolipin. The negatively charged surface locks the peptide onto the surface by electrostatic interactions and triggers α-helical secondary structure changes.

seen in the ^{1}H NMR and ^{31}P NMR results, Bax-α1 interacts strongly with the glycerol and the headgroup regions of the membrane and especially with cardiolipin, without any pronounced perturbation of the hydrophobic bilayer core. This observation can directly be connected to the fact the two phosphate groups of cardiolipin are exposed to the peptide, triggering a strong electrostatic interaction with the three positive charges of Bax-α1. Therefore, one can assume that cardiolipin has the possibility to trap Bax-α1. Furthermore, inspecting the ^{31}P NMR resonance integrals, as summarized in Table 2, cardiolipin appears to be the most involved lipid in the 4th component population, the so-called peptide-interacting lipid pool. Only 24% of the total cardiolipin amount remains in a "free" phase compared to 42% or 44% for POPC or POPE, respectively. Bax-α1 preferential interaction with cardiolipin is further supported by the chemical shift of the "free" lipids towards a more neutral surface membrane [25,40]. Since the major difference between the two models is the presence of an anionic lipid, one can conclude that peptide insertion in OM is driven by a hydrophobic mechanism.

4.2. Peptide plasticity modulated by its environment

Neutral membranes promote an increase in β-sheet fraction of Bax-α1 which is most likely due to hydrophobic interactions caused by the reduced freedom of the beta-sheet/random coil equilibrium and peptide insertion in the hydrophobic core of the bilayers. At high peptide concentration, the peptide is forced into contact with the membrane surface as seen in the NMR experiments. This reduced freedom triggers the accumulation of the peptide and its structural change into beta-sheet features (+20%) whose hydrophobic nature can drive extensive insertion. ATR experiments of the same peptide/membrane systems support the finding that Bax-α1 inserts in the membrane matrix as an anti-parallel β-sheet at high concentration. Upon interaction with CS membranes, Bax-α1 is able to change its secondary structure between β-sheet and α-helix; an observation which is in accordance with our previous study where negatively charged membranes induced helical formation of Bax-α1 depending on the surface charge potential [21]. However, differences between DMPC and POPC/POPE are noticeable. Indeed, Bax-α1 seems to have less affinity for DMPC, inducing less structural changes, than with OM vesicles. It might come from the fact that DMPC bilayers are more ordered in the Lα phase than POPC bilayers at the same temperature, and/or lower thickness of the hydrophobic core of DMPC membrane that would prevent the insertion of the peptide and therefore less structural changes, a phenomenon known as hydrophobic mismatch between membranes and spanning peptides [39,41,42]. Indeed, as seen in a recent study on a cell penetrating peptide, DMPC forced a more parallel orientation of the peptide, meaning less energetically favorable, compared to POPC due to hydrophobic mismatch [39]. The remarkable ability of Bax-α1 to modify its secondary structure according to the lipid environment, the propensity of cardiolipin to trap the N terminal of Bax are two major findings for a further elucidation of the regulation of mitochondrial apoptosis and will therefore be discussed in the following section.

4.3. Potential biological implication for Bax targeting mitochondria

One of the key events in the regulation of apoptosis via the mitochondrial pathway is the translocation of Bax to the mitochondrion [7,14,43]. During this process pro- and anti-apoptotic proteins are strongly anchored at the mitochondrial membrane system in order to regulate the fate of the cell but one does not know how the regulation takes place. Indeed, there is a debate on whether Bax can form pores on

its own or alternatively can interact with native pores [44–47]. Furthermore, the N terminal *versus* the C terminal involvement in the Bax location is still versatile [15–17,48]. However, there seems to be a consensus that a specific lipid environment is directly involved into insertion and/or regulation of the Bax protein [18,45,49–53].

We found that the potential addressing sequence of Bax has a low affinity for the OM membranes. But it has the ability to insert if a strong self-association occurs before entering in close contact. Interestingly, it has been shown that adding the first helix of Bax to a cytosolic protein lead to its translocation towards mitochondrial membranes. And not surprisingly, a L26G mutation decreased the association efficiency of Bax-α1-protein to mitochondria [48]. These findings agree with the results presented here, since the mutation decreases the hydrophobicity of the N terminal and therefore reduces its insertion ability. Meanwhile, it stays unlikely that Bax recognizes the OM by its N terminal part considering that no strong auto-association of the full protein in solution has been found previously. However, we report that cardiolipin is required for the binding of the first helix of Bax protein to mitochondrial membrane which can be the first step in Bax addressing to mitochondria. It explains the given role of cardiolipin in apoptosis regulation. Indeed, CL was shown to be essential for Bax activation; depletion of CL in the OM would increase the cell resistance to apoptosis induction or that Bax–Bid–cardiolipin complexes are known to promote the release of cytochrome *c* or dextran molecules in membrane models [9,18,50,54]. However, from our results, the insertion of Bax via its N terminal is either not promoted by interactions with contact sites or it is driven by another part of the protein. The N terminal could act as a pure targeting sequence as previously proposed, while the subsequent insertion steps would be promoted by other protein domains [16,43,55]. This would also explain recent contradictory findings that either the C terminal or the N Terminal of Bax is responsible for its anchoring into mitochondria [16,17,48]. The specific interaction between cardiolipin and Bax-α1, as demonstrated herein, would then be required for addressing Bax to the correct location in the mitochondria, and the presence of cardiolipin in the OM could act as a strong signaling for Bax translocation.

Acknowledgements

We are grateful to Axelle Grelard, Bernard Desbat, (Université Bordeaux 1-ENITAB, France) and Göran Lindblom, Lennart Johansson and Eric Rosenbaum (Umeå University) for all their support. This work was supported by Knut and Alice Wallenberg Foundation, Carl Kempe Foundation, Swedish Research Council, Umeå University Insamlingsstiftelse and the Centre National de la Recherche Scientifique (CNRS). The Aquitaine region is acknowledged for equipment funding and the universities of Bordeaux 1 and Umeå for setting up a co-tutoring Ph.D. program.

Appendix A. Supplementary data

Supplementary data associated with this article can be found, in the online version, at doi:10.1016/j.bbamem.2008.12.014.

References

[1] H. Okada, T.W. Mak, Pathways of apoptotic and non-apoptotic death in tumour cells, Nat. Rev., Cancer 4 (2004) 592–603.
[2] C.B. Thompson, Apoptosis in the pathogenesis and treatment of disease, Science 267 (1995) 1456–1462.
[3] J.F. Kerr, A.H. Wyllie, A.R. Currie, Apoptosis: a basic biological phenomenon with wide-ranging implications in tissue kinetics, Br. J. Cancer 26 (1972) 239–257.
[4] S. Cory, J.M. Adams, The BCL2 family: regulators of the cellular life-or-death switch, Nat. Rev., Cancer 2 (2002) 647–656.
[5] M.O. Hengartner, The biochemistry of apoptosis, Nature 407 (2000) 770–776.
[6] G. Kroemer, Mitochondrial control of apoptosis: an overview, Biochem. Soc. Symp. 66 (1999) 1–15.
[7] D.M. Finucane, E. Bossy-Wetzel, N.J. Waterhouse, T.G. Cotter, D.R. Green, Bax-induced caspase activation and apoptosis via cytochrome *c* release from mitochondria is inhibitable by Bcl-xL, J. Biol. Chem. 274 (1999) 2225–2233.
[8] E. Jacotot, P. Costantini, E. Laboureau, N. Zamzami, S.A. Susin, G. Kroemer, Mitochondrial membrane permeabilization during the apoptotic process, Ann. N. Y. Acad. Sci. 887 (1999) 18–30.
[9] J.M. Jurgensmeier, Z. Xie, Q. Deveraux, L. Ellerby, D. Bredesen, J.C. Reed, Bax directly induces release of cytochrome *c* from isolated mitochondria, Proc. Natl. Acad. Sci. U. S. A. 95 (1998) 4997–5002.
[10] Y.T. Hsu, K.G. Wolter, R.J. Youle, Cytosol-to-membrane redistribution of Bax and Bcl-X-L during apoptosis, Proc. Natl. Acad. Sci. U. S. A 94 (1997) 3668–3672.
[11] G. Kroemer, J.C. Reed, Mitochondrial control of cell death, Nat. Med. 6 (2000) 513–519.
[12] X. Roucou, J.C. Martinou, Conformational change of Bax: a question of life or death, Cell Death Differ. 8 (2001) 875–877.
[13] M. Suzuki, R.J. Youle, N. Tjandra, Structure of Bax: coregulation of dimer formation and intracellular localization, Cell 103 (2000) 645–654.
[14] I.S. Goping, A. Gross, J.N. Lavoie, M. Nguyen, R. Jemmerson, K. Roth, S.J. Korsmeyer, G.C. Shore, Regulated targeting of BAX to mitochondria, J. Cell Biol. 143 (1998) 207–215.
[15] P.F. Cartron, M. Priault, L. Oliver, K. Meflah, S. Manon, F.M. Vallette, The N-terminal end of Bax contains a mitochondrial-targeting signal, J. Biol. Chem. 278 (2003) 11633–11641.
[16] A.J. Valentijn, J.P. Upton, N. Bates, A.P. Gilmore, Bax targeting to mitochondria occurs via both tail anchor-dependent and -independent mechanisms, Cell Death Differ. (2008).
[17] L. Lalier, P.F. Cartron, P. Juin, S. Nedelkina, S. Manon, B. Bechinger, F.M. Vallette, Bax activation and mitochondrial insertion during apoptosis, Apoptosis 12 (2007) 887–896.
[18] S. Lucken-Ardjomande, S. Montessuit, J.C. Martinou, Contributions to Bax insertion and oligomerization of lipids of the mitochondrial outer membrane, Cell Death Differ. 15 (2008) 929–937.
[19] D. Ardail, J.P. Privat, M. Egret-Charlier, C. Levrat, F. Lerme, P. Louisot, Mitochondrial contact sites. Lipid composition and dynamics, J. Biol. Chem. 265 (1990) 18797–18802.
[20] M. Schlame, D. Rua, M.L. Greenberg, The biosynthesis and functional role of cardiolipin, Prog. Lipid Res. 39 (2000) 257–288.
[21] M.A. Sani, C. Loudet, G. Grobner, E.J. Dufourc, Pro-apoptotic bax-alpha1 synthesis and evidence for beta-sheet to alpha-helix conformational change as triggered by negatively charged lipid membranes, J. Pept. Sci. 13 (2006) 100–106.
[22] N. Sreerama, R.W. Woody, A self-consistent method for the analysis of protein secondary structure from circular dichroism, Anal. Biochem. 209 (1993) 32–44.
[23] N. Sreerama, R.W. Woody, Estimation of protein secondary structure from circular dichroism spectra: comparison of CONTIN, SELCON, and CDSSTR methods with an expanded reference set, Anal. Biochem. 287 (2000) 252–260.
[24] N. Sreerama, R.W. Woody, Analysis of protein CD spectra: comparison of CONTIN, SELCON3, and CDSSTR methods in CDPro software, Biophys. J. 78 (2000) 334A.
[25] F. Lindstrom, P.T. Williamson, G. Grobner, Molecular insight into the electrostatic membrane surface potential by 14n/31p MAS NMR spectroscopy: nociceptin-lipid association, J. Am. Chem. Soc. 127 (2005) 6610–6616.
[26] J.H. Davis, Deuterium magnetic resonance study of the gel and liquid crystalline phases of dipalmitoyl phosphatidylcholine, Biophys. J. 27 (1979) 339–358.
[27] E. Goormaghtigh, V. Cabiaux, J.M. Ruysschaert, Secondary structure and dosage of soluble and membrane-proteins by attenuated total reflection Fourier-transform infrared-spectroscopy on hydrated films, Eur. J. Biochem. 193 (1990) 409–420.
[28] E. Goormaghtigh, V. Raussens, J.M. Ruysschaert, Attenuated total reflection infrared spectroscopy of proteins and lipids in biological membranes, Biochim. Biophys. Acta 1422 (1999) 105–185.
[29] E. Goormaghtigh, V. Cabiaux, J.M. Ruysschaert, Determination of soluble and membrane protein structure by Fourier transform infrared spectroscopy. III. Secondary structures, Subcell. Biochem. 23 (1994) 329–450.
[30] L.K. Tamm, S.A. Tatulian, Infrared spectroscopy of proteins and peptides in lipid bilayers, Q. Rev. Biophys. 30 (1997) 365–429.
[31] M. Bokvist, F. Lindstrom, A. Watts, G. Grobner, Two types of Alzheimer's beta-amyloid (1–40) peptide membrane interactions: aggregation preventing transmembrane anchoring versus accelerated surface fibril formation, J. Mol. Biol. 335 (2004) 1039–1049.
[32] E.J. Dufourc, C. Mayer, J. Stohrer, G. Althoff, G. Kothe, Dynamics of phosphate head groups in biomembranes — comprehensive analysis using P-31 nuclear-magnetic-resonance lineshape and relaxation-time measurements, Biophys. J. 61 (1992) 42–57.
[33] E.J. Dufourc, C. Mayer, J. Stohrer, G. Kothe, P-31 and H-1-NMR pulse sequences to measure lineshapes, T1z and T2e relaxation-times in biological-membranes, J. Chim. Phys. Pcb 89 (1992) 243–252.
[34] T.L. Pukala, M.P. Boland, J.D. Gehman, L. Kuhn-Nentwig, F. Separovic, J.H. Bowie, Solution structure and interaction of cupiennin 1a, a spider venom peptide, with phospholipid bilayers, Biochemistry 46 (2007) 3576–3585.
[35] B.B. Bonev, W.C. Chan, B.W. Bycroft, G.C. Roberts, A. Watts, Interaction of the lantibiotic nisin with mixed lipid bilayers: a 31P and 2H NMR study, Biochemistry 39 (2000) 11425–11433.
[36] K. Nomura, G. Corzo, T. Nakajima, T. Iwashita, Orientation and pore-forming mechanism of a scorpion pore-forming peptide bound to magnetically oriented lipid bilayers, Biophys. J. 87 (2004) 2497–2507.
[37] S. Castano, B. Desbat, Structure and orientation study of fusion peptide FP23 of gp41 from HIV-1 alone or inserted into various lipid membrane models (mono-,

bi- and multibi-layers) by FT-IR spectroscopies and Brewster angle microscopy, Biochim. Biophys. Acta 1715 (2005) 81–95.
[38] L. Lins, R. Brasseur, M. Rosseneu, C.Y. Yang, D.A. Sparrow, J.T. Sparrow, A.M. Gotto Jr., J.M. Ruysschaert, Structure and orientation of apo B-100 peptides into a lipid bilayer, J. Protein Chem. 13 (1994) 77–88.
[39] A. Ramamoorthy, S.K. Kandasamy, D.K. Lee, S. Kidambi, R.G. Larson, Structure, topology, and tilt of cell-signaling peptides containing nuclear localization sequences in membrane bilayers determined by solid-state NMR and molecular dynamics simulation studies, Biochemistry 46 (2007) 965–975.
[40] A. Ramamoorthy, S. Thennarasu, A. Tan, D.K. Lee, C. Clayberger, A.M. Krensky, Cell selectivity correlates with membrane-specific interactions: a case study on the antimicrobial peptide G15 derived from granulysin, Biochim. Biophys. Acta 1758 (2006) 154–163.
[41] J.A. Killian, Hydrophobic mismatch between proteins and lipids in membranes, Biochim. Biophys. Acta 1376 (1998) 401–415.
[42] J.A. Killian, I. Salemink, M.R. de Planque, G. Lindblom, R.E. Koeppe Jr., D.V. Greathouse, Induction of nonbilayer structures in diacylphosphatidylcholine model membranes by transmembrane alpha-helical peptides: importance of hydrophobic mismatch and proposed role of tryptophans, Biochemistry 35 (1996) 1037–1045.
[43] E. Er, L. Oliver, P.F. Cartron, P. Juin, S. Manon, F.M. Vallette, Mitochondria as the target of the pro-apoptotic protein Bax, Biochim. Biophys. Acta 1757 (2006) 1301–1311.
[44] C.P. Baines, R.A. Kaiser, T. Sheiko, W.J. Craigen, J.D. Molkentin, Voltage-dependent anion channels are dispensable for mitochondrial-dependent cell death, Nat. Cell Biol. 9 (2007) 550–555.
[45] G. Basanez, J.C. Sharpe, J. Galanis, T.B. Brandt, J.M. Hardwick, J. Zimmerberg, Bax-type apoptotic proteins porate pure lipid bilayers through a mechanism sensitive to intrinsic monolayer curvature, J. Biol. Chem. 277 (2002) 49360–49365.
[46] S. Shimizu, A. Konishi, T. Kodama, Y. Tsujimoto, BH4 domain of antiapoptotic Bcl-2 family members closes voltage-dependent anion channel and inhibits apoptotic mitochondrial changes and cell death, Proc. Natl. Acad. Sci. U. S. A 97 (2000) 3100–3105.
[47] S. Shimizu, M. Narita, Y. Tsujimoto, Bcl-2 family proteins regulate the release of apoptogenic cytochrome *c* by the mitochondrial channel VDAC, Nature 399 (1999) 483–487.
[48] P.F. Cartron, C. Moreau, L. Oliver, E. Mayat, K. Meflah, F.M. Vallette, Involvement of the N-terminus of Bax in its intracellular localization and function, FEBS Lett. 512 (2002) 95–100.
[49] J.A. Yethon, R.F. Epand, B. Leber, R.M. Epand, D.W. Andrews, Interaction with a membrane surface triggers a reversible conformational change in Bax normally associated with induction of apoptosis, J. Biol. Chem. 278 (2003) 48935–48941.
[50] T. Kuwana, M.R. Mackey, G. Perkins, M.H. Ellisman, M. Latterich, R. Schneiter, D.R. Green, D.D. Newmeyer, Bid, Bax, and lipids cooperate to form supramolecular openings in the outer mitochondrial membrane, Cell 111 (2002) 331–342.
[51] R.F. Epand, J.C. Martinou, S. Montessuit, R.M. Epand, Transbilayer lipid diffusion promoted by Bax: implications for apoptosis, Biochemistry 42 (2003) 14576–14582.
[52] J. Jiang, Z. Huang, Q. Zhao, W. Feng, N.A. Belikova, V.E. Kagan, Interplay between bax, reactive oxygen species production, and cardiolipin oxidation during apoptosis, Biochem. Biophys. Res. Commun. 368 (2008) 145–150.
[53] B. Leber, J. Lin, D.W. Andrews, Embedded together: the life and death consequences of interaction of the Bcl-2 family with membranes, Apoptosis 12 (2007) 897–911.
[54] Q. Van, J. Liu, B. Lu, K.R. Feingold, Y. Shi, R.M. Lee, G.M. Hatch, Phospholipid scramblase-3 regulates cardiolipin de novo biosynthesis and its resynthesis in growing HeLa cells, Biochem. J. 401 (2007) 103–109.
[55] H. Arokium, N. Camougrand, F.M. Vallette, S. Manon, Studies of the interaction of substituted mutants of BAX with yeast mitochondria reveal that the C-terminal hydrophobic alpha-helix is a second ART sequence and plays a role in the interaction with anti-apoptotic BCL-x(L), J. Biol. Chem. 279 (2004) 52566–52573.